

Microscopic and macroscopic models of photo-induced volume changes in amorphous selenium

Rozália Lukács · József Hegedüs · Sandor Kugler

Received: 20 July 2007 / Accepted: 1 October 2007 / Published online: 25 October 2007
© Springer Science+Business Media, LLC 2007

Abstract We have proposed a new explanation for the photo-induced volume changes in chalcogenide glasses. We have found that the covalent bond breaking occurs in these glasses with excited electrons, whereas holes contribute to the formation of inter-chain bonds. We have calculated the charge distribution in a-Se, too.

1 Introduction

During bandgap illumination, chalcogenide glasses exhibit various changes in structural and electronic properties like photo-induced volume change, photodarkening, and photo-induced change in the phase state (photo-crystallization and photo-amorphization) [1]. The phase change materials are one of the most exiting recent developments. Phase change memory is based on transition between nanocrystalline and glassy chalcogenides. The macroscopic picture of chalcogenide memory operations is simple: heating and fast or slow cooling of the liquid leads to reaching phases with different electrical resistivities. Rewritable optical data recording is the recent most important applications of thin chalcogenide films. Dominant materials for them are Ge Sb Te alloys today.

These phenomena do not occur in any other amorphous semiconductors. The microscopic structural changes are facilitated by two factors common to chalcogenide glasses: the low average coordination number and the structural

freedom of the non-crystalline state. During illumination some of the films can expand (a-As₂S₃, a-As₂Se₃, etc.), and the others shrink (a-GeS₂, a-GeSe₂, etc.) [2]. Several investigations have been carried out in order to provide an explanation of these phenomena [3–10]. We proposed a simple, unified description of the photo-induced volume changes in chalcogenides based on tight-binding (TB) molecular dynamics (MD) simulations of amorphous selenium [8]. We have found that the microscopic rearrangements in the structure (like bond breaking and bond formation) are responsible for the macroscopic volume change under illumination. The first in situ surface height measurement [11] on amorphous selenium was carried out recently and supports our proposed mechanism.

2 Computer simulation background

We have recently developed a molecular dynamics computer code (ATOMDEP program package) to simulate the preparation procedures of real amorphous structures (growth by atom-by-atom deposition on a substrate and rapid quenching) [12–16]. Standard velocity Verlet algorithm was applied in our MD simulations in order to follow the atomic scale motions. To control the temperature we applied the velocity-rescaling method. We chose $\Delta t = 1$ fs or 2 fs for the time step, depending on the temperature. In our works the growth of amorphous carbon [12], silicon [13, 14] and selenium [15, 16] films were simulated by this MD method. This computer code is convenient to investigate photo-induced volume changes as well if the built-in atomic interaction can handle the photo-excitation. For calculating the inter-atomic forces in a-Se we used tight-binding [16, 17] and self-consistent tight-binding (SCF-TB) [16, 18] models. The TB parameterization [17] has

R. Lukács · J. Hegedüs · S. Kugler (✉)
Department of Theoretical Physics, Budapest University of
Technology and Economics, Budafoki ut 8, Budapest 1521,
Hungary
e-mail: kugler@eik.bme.hu

been introduced for disordered selenium following the techniques developed by Goodwin et al. [19].

3 Sample preparation

Hundred and sixty-two atom glassy networks in rectangular box were fabricated with periodic boundary conditions in two dimensions [x,y]. The samples were open in the z-direction. When we illuminated the cell, it could expand or shrink into the open direction if did. The volume changes in the sample could be derived by measuring the distance between atoms at the two open ends (see arrow in Fig. 1).

The sample had an initial density of 4.33 g/cm^3 . We prepared our samples from liquid phase by rapid quenching. Our ‘cook and quench’ sample preparation procedure was as follows (see Fig. 2): first we set the temperature of the system to 5,000 K for the first 300 MD steps. During the following 2,200 MD steps, we decreased linearly the

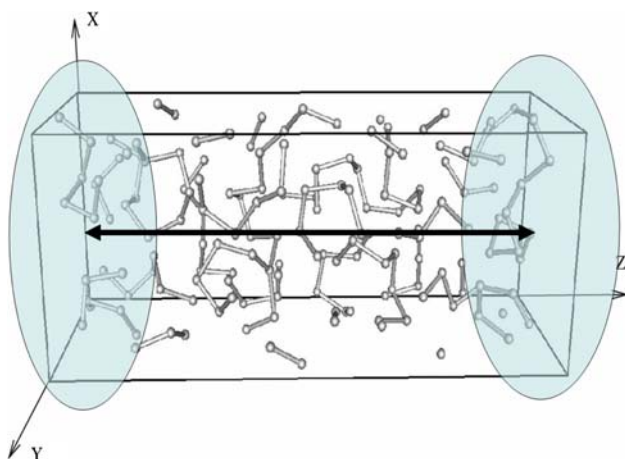


Fig. 1 Snapshot of a final glassy selenium network. The sample can move in z-direction

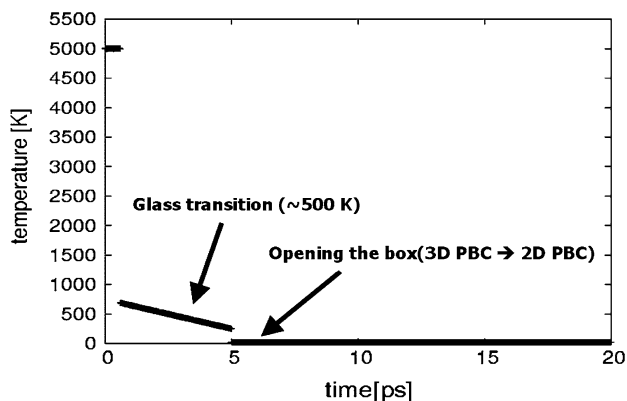


Fig. 2 Temperature as a function of time during the sample preparation

temperature from 700 K to 250 K, driving the sample through the glass transition and reaching the condensed phase. Then we set the final temperature to 20 K and relaxed the sample for 500 (1 ps) MD steps. The closed box was opened in the z-direction at the 3,000th MD step. We thus obtained two surfaces with increased number of onefold coordinated atoms. This final topology corresponded to a thin-film structure. A typical configuration can be seen in Fig. 1.

Samples prepared at 20 K had final densities from 3.95 g/cm^3 upto 4.19 g/cm^3 . The number of coordination defects ranged from 3% up to 12%. Most of these defects were located on the surfaces. The structure mainly consisted of branching chains, but some rings could also be found. The samples were accepted if the volume fluctuation was less than 0.5% in 60 picoseconds. We prepared altogether 30 samples, and 17 were considered to be stable and useful for further studies. A radial distribution function of a representative sample can be seen in Fig 3.

In our Molecular Dynamics (MD) simulation on a-Se [8], we assumed that immediately after a photon absorption the electron and the hole become separated in space on a femtosecond time scale [20]. This effect is applied in our everyday life using copy machines, where the cylinder is made from selenium. Therefore, excited electrons and created holes can be treated independently in our cluster calculations. We ran two sets of simulations: first, to model the excited electron creation, we put an extra electron into the Lowest Unoccupied Molecular Orbital (LUMO), and second, we annihilated an electron in the Highest Occupied Molecular Orbital, HOMO (hole creation). We neglect the Coulomb interaction between electrons and holes. In our approach, excitons do not play any role during the photo-induced volume changes.

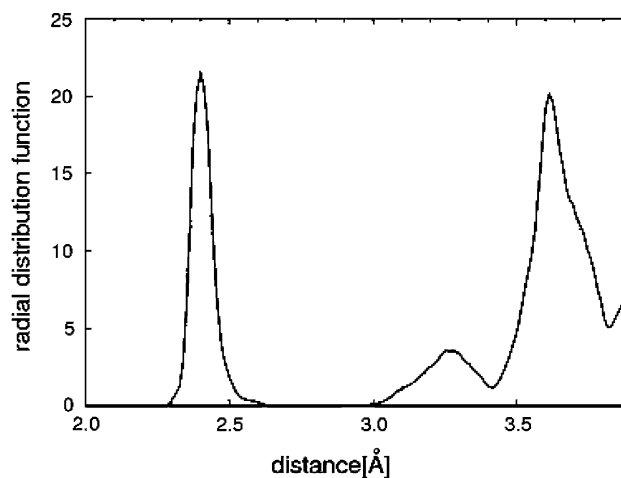


Fig. 3 Radial distribution function of amorphous selenium network in function of atomic distances. The model was prepared by MD simulation at 20 K

4 Electron excitation and hole creation

When an additional electron was put on the LUMO in the majority of cases, a covalent bond between twofold and threefold coordinated atoms was broken ($C2 + C3 \geq C1 + C2$). This effect causes a macroscopic volume expansion. Release of excitation restores all bond lengths to their original value. More interesting results were obtained during hole creation. We observed that inter-chain bonds were formed after creating a hole, and they cause a contraction of the sample. This always happens near to atoms where the HOMO is localized. Since the HOMO is usually localized in the vicinity of a onefold coordinated atom, the inter-chain bond formation often takes place between a onefold coordinated atom and a twofold coordinated atom ($C\{1,0\} + C\{2,0\} \geq C\{1,1\} + C\{2,1\}$, where the second number means the number of inter-chain bonds). However, sometimes we also observed the formation of inter-chain bonds between two twofold coordinated atoms ($C\{2,0\} + C\{2,0\} \geq C\{2,1\} + C\{2,1\}$).

5 Charge distributions

A covalent bond between twofold and threefold coordinated atoms was broken ($C2 + C3 \geq C1 + C2$) in the majority. In that occasion we started to investigate the charge distribution in our a-Se models. Two different methods were applied for this purpose i.e. Density Functional Theory (DFT) and Tight-Binding model. Figure 4 displays the charge distributions using DFT GGA calculation on 162 atom clusters. Basically, the absolute value of charge accumulations on the twofold coordinated atoms are less than 0.1 electron units. Furthermore we can observe some larger charge accumulations in both directions as the two insets show. The larger positive charge accumulation belongs to the threefold coordinated atoms, while the negatively charged atoms are onefold coordinated.

Similar effect was observed using TB model. The only difference between charges calculated by TB and DFT is the values because in the TB case the charges are a little bit larger (see Figs. 4. and 5).

In stable condensed phases the selenium atoms (and other chalcogenide elements) form covalent bonds with two nearest neighbours in accordance with the 8-N rule. These atoms have six electrons in the outermost shell with a configuration of s^2p^4 . Electrons in s states do not participate in bonding since these states have energies well below the p states. Two covalent bonds are formed between chalcogen atoms by two p electrons, but the other electron pair—also called a lone pair (LP)—remains in a non-bonding state. If there is a coordination defect or doping the 8-N rule must be broken. No electron-spin-resonance (ESR) signal

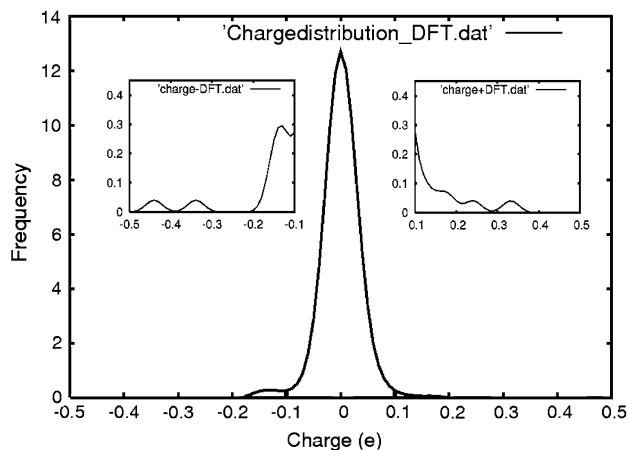


Fig. 4 Charge distribution in a-Se calculated by DFT method. Two insets display the atomic charges on onefold and threefold coordinated atoms

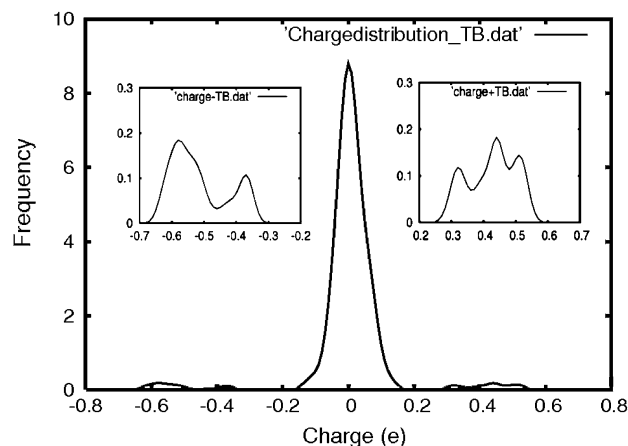


Fig. 5 Charge distribution in a-Se calculated by TB method. Two insets display the atomic charges on onefold and threefold coordinated atoms. In this case the charges are a little bit larger than in DFT calculations can be found

has been observed in a-Se. A possible explanation of this phenomenon is that the defects are not neutral: onefold coordinated atoms are negatively charged ($C1$) and threefold coordinated atoms are positively charged ($C3$) which are called valence alternation pairs (VAP's).

Our calculations which do not contain phonon-electron interaction suggest that the threefold coordinated atoms lost an electron and these electrons are transferred to the end of chains causing a negatively charged end.

6 Macroscopic models. Kinetics of volume change

The light induced volume expansion and volume shrinkage in amorphous selenium simultaneously exist, so that they are additive quantities. The expansion in thickness d_e is proportional to the number of excited electrons n_e

($d_e = \beta_e n_e$), while the shrinkage d_h is proportional to the number of created holes n_h ($d_h = \beta_h n_h$). The parameter β_e (β_h) is the average thickness change caused by an excited electron (hole). The macroscopic time dependent thickness change is equal to

$$\Delta(t) = \beta_e n_e(t) - \beta_h n_h(t) \quad (1)$$

where $\Delta(t)$, $n_e(t)$, and $n_h(t)$ are sum of stepwise functions.

Assuming $n_e(t) = n_h(t) = n(t)$ we get

$$\Delta(t) = (\beta_e - \beta_h)n(t) = \beta_\Delta n(t) \quad (2)$$

where β_Δ is a characteristic constant of the chalcogenide glasses related to the photo-induced volume (thickness) change. The sign of this parameter governs whether the material shrinks or expands. The number of electrons excited and holes created is proportional to the time during illumination. Their time independent generation rate G depends on the photon absorption coefficient. Recombination is a reverse process. The number of electron-hole recombination events depends on the time and on the number of excited electrons and holes. A rate equation for this dominant process can be written as follows

$$dn_e/dt = G - C n_e(t) n_h(t), \quad (3)$$

where C is the recombination rate. Using $n_e(t) = n_h(t) = n(t)$ and $\Delta(t) = \beta_\Delta n(t)$, we obtain an equation for the time dependent volume change, namely

$$d\Delta(t)/dt = G\beta_\Delta - (C/\beta_\Delta)\Delta^2(t). \quad (4)$$

The solution of this nonlinear differential equation is given by (using: $G' = G\beta_\Delta$; $C' = C/\beta_\Delta$)

$$\Delta(t) = (G'/C')^{1/2} \tanh((G'C')^{1/2}t). \quad (5)$$

In the steady state case ($t = \infty$)

$$\Delta(t = \infty) = (G'/C')^{1/2} = a. \quad (6)$$

$\Delta(t = \infty) = a$ is a well-known measurable value from experiments ($\Delta(t) = a \tanh((G'C')^{1/2}t)$). After the light is turned off. Eq. (4) reduces to ($G = 0$)

$$d\Delta(t)/dt = -C'\Delta^2(t) \quad (7)$$

with the solution

$$\Delta(t) = a/(aC't + 1). \quad (8)$$

We have only one fitting parameter (only C' because $G'/C' = a^2$) and two different curves to fit using this parameter! Fig. 6 displays the best fit for the photoinduced volume expansion of a-Se glass during illumination. The dashed line shows the measured volume including fluctuations while the solid line was drawn using our model. The horizontal dashed line is the upper limit of the volume expansion ($\Delta(t = \infty) = a$). The measured volume shrinkage of a-Se (dotted line) and the fitted curve (solid

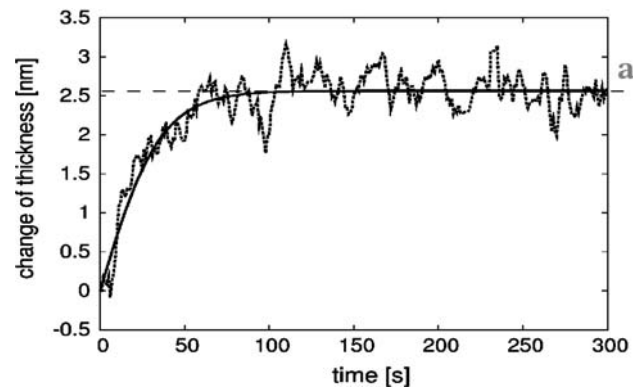


Fig. 6 Time development of the measured volume expansion in amorphous selenium (dotted line) and its fit using our model (solid line)

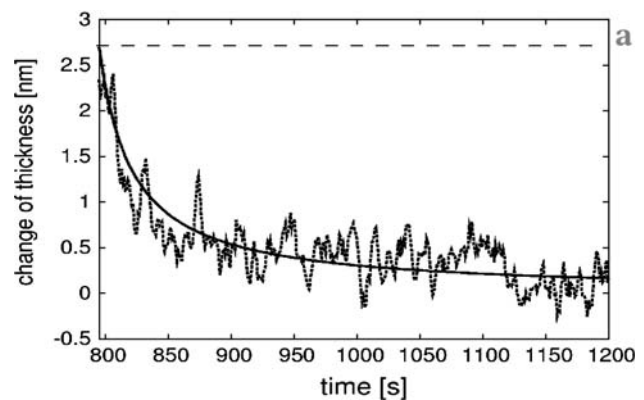


Fig. 7 The measured shrinkage of a-Se (dotted line) and the fitted curve (solid line) after switching off the illumination

line) are shown after switching off the illumination in Fig. 7.

This kinetics is not a stretched exponent governed process which is usually expected for amorphous materials. In our microscopic model we applied a uniform β_Δ for explanation the photoinduced volume change. In order to give a detailed description we applied a distribution for β_Δ . Furthermore we used Debye type exponential expansion and shrinkage with different relaxation time instead of stepwise description. We were not able to obtain stretched exponent function for the time development of photoinduced volume change.

7 Summary

In summary, we have proposed a comprehensive explanation of photo-induced volume changes in chalcogenide glasses, which can simultaneously describe photo-induced shrinkage and expansion. This phenomenon is unique to amorphous chalcogenides because of the twofold coordination of the chalcogenide atoms, which provides structural flexibility. We found covalent bond breaking in systems

with excited electrons, whereas holes contribute to the formation of inter-chain bonds in the vicinity where these excited electrons and holes are localized. The interplay between photo-induced bond breaking and inter-chain bond formation leads to either volume expansion or shrinkage. Our comprehensive microscopic explanation of the photo-induced volume change is in an excellent agreement with the first in situ surface height measurements in amorphous selenium. Our calculations of atomic charge accumulation provide a direct evidence of existences of positively charged (C3) and negatively charged (C1) atomic sites in a-Se network. Methods we used for this purpose do not contain phonon-electron interaction.

Acknowledgments This work has been supported by the OTKA Fund (Grants No. T048699). Simulations have been carried out using computer resources provided to us by the Tokyo Polytechnic University. We are indebted to Prof. Takeshi Aoki for this possibility. We also thank the John von Neumann Institut für Computing (NIC), Forschungszentrum Jülich, Germany, for cpu time grants on their supercomputer systems for our DFT calculations. We would also like to acknowledge many valuable discussions with K. Kohary at the University of Oxford and Prof. Koichi Shimakawa (Gifu Univ. Japan).

References

1. J. Singh (ed.), *Optical Properties of Condensed Matter and Applications* (John Wiley & Sons, UK, 2006)
2. Y. Kuzukawa, A. Ganjoo, K. Shimakawa, *J. Non-Cryst. Solids* **227**, 715 (1998) and *Philos. Mag. B* **79**, 249 (1999)
3. V. Palyok, I.A. Szabo, D.L. Beke, A. Kikineshi, *Appl. Phys. A* **74**, 683 (2001)
4. K. Shimakawa, N. Yoshida, A. Gahjoo, A. Kuzukawa, J. Singh, *Philos. Mag. Lett.* **77**, 153 (1998)
5. H. Fritzsche, *Solid State Commun.* **99**, 153 (1996)
6. A.V. Kolobov, H. Oyanagi, K. Tanaka, Ke. Tanaka, *Phys. Rev. B* **55**, 726 (1997)
7. X. Zhang, D.A. Drabold, *Phys. Rev. Lett.* **83**, 5042 (1999)
8. J. Hegedüs, K. Kohary, D.G. Pettifor, K. Shimakawa, S. Kugler, *Phys. Rev. Lett.* **95**, 206803 (2005)
9. T. Uchino, D.C. Clary, S.R. Elliott, *Phys. Rev. Lett.* **85**, 3305 (2000)
10. A. Reznik, B.J.M. Lui, V. Lyubin, M. Klebanov, Y. Ohkawa, T. Matsubara, K. Miyakawa, M. Kubota, K. Tanioka, T. Kawai, J.A. Rowlands, *J. Non-Cryst. Solids* **352**, 1595 (2006)
11. Y. Ikeda, K. Shimakawa, *J. Non-Cryst. Solids* **338**, 539 (2004)
12. K. Kohary, S. Kugler, *Phys. Rev. B* **63**, 193404 (2001)
13. S. Kugler, K. Kohary, K. Kádas, L. Pusztai, *Solid State Commun.* **127**, 305 (2003)
14. K. Kohary, S. Kugler, *Mol. Simul.* **30**, 17 (2004)
15. J. Hegedüs, K. Kohary, S. Kugler, *J. Non-Cryst. Solids* **338**, 283 (2004)
16. J. Hegedüs, S. Kugler, *J. Phys.: Condens. Matter* **17**, 6459 (2005)
17. D. Molina, E. Lomba, *Phys. Rev. B* **60**, 6372 (1999)
18. E. Lomba, D. Molina, M. Alvarez, *Phys. Rev. B* **61**, 9314 (2000)
19. L. Goodwin, A.J. Skinner, D.G. Pettifor, *Europhys. Lett.* **9**, 701 (1989)
20. D. Moses, *Phys. Rev. B* **53**, 4462 (1996)